Available online at www.sciencedirect.com
ScienceDirect
Journal of Molecular Catalysis A: Chemical 266 (2007) 239–248
JOURNAL OF MOLECULAR CATALYSIS A: CHEMICAL
www.elsevier.com/locate/molcata

Iron-assisted, base-catalyzed biomimetic activation of dioxygen by dioximatoiron(II) complexes Kinetics and mechanism of model catecholase activity

Zoltán May [a], László I. Simándi [a,*], Attila Vértes [b]

[a] *Institute of Surface Science and Catalysis, Chemical Research Center, Hungarian Academy of Sciences, H-1525 Budapest, P.O. Box 17, Hungary*
[b] *Laboratory of Nuclear Chemistry, L. Eötvös University, Budapest, Hungary*

Received 9 October 2006; accepted 7 November 2006
Available online 16 November 2006

Abstract

The dioximatoiron complexes $[Fe(Hdmed)]^+$, $[Fe(Hdmpd)]^+$ and $[Fe(H_2dmdt)]^{2+}$ catalyze the oxidation of 3,5-di-*tert*-butylcatechol (H_2dtbc) by O_2 to the corresponding *o*-benzoquinone (dtbq) at room temperature in MeOH solution. The reaction was followed by measuring the rate of dioxygen absorption as a function of catalyst, substrate and dioxygen concentration. Kinetic measurements reveal first-order dependence on the catalyst and O_2 concentration and saturation type behavior with respect to the substrate. The proposed reaction mechanism involves prior binding of the substrate H_2dtbc and O_2 to the iron complex, forming a ternary active intermediate, decomposing in the rate-limiting step to a semiquinonato anion radical ($dbsq^{\bullet -}$), detected by ESR spectroscopy. It is then rapidly oxidized to the dtbq product. Added triethylamine accelerates the reaction to an extent much greater than that expected from the parallel base-catalyzed oxidation route. The kinetic behavior is similar to the TEA-free systems except for a saturation type dependence on TEA. This feature is due to a novel iron-enhanced oxidation path in which $Hdtbc^-$ binds O_2 to form the hydroperoxide $HdtbcO_2^-$, coordinating to the iron(II) complexes as a hydroperoxo ligand. Subsequently, the hydroperoxo complex eliminates $dbsq^-$, which is directly oxidized by O_2 to dtbq. According to Mössbauer spectroscopy, the catalyst species are predominantly low-spin iron(II) complexes.

Keywords: Biomimetic oxidation; Dioximatoiron(II); 3,5-di-*tert*-Butylcatechol; Iron-enhanced oxidation; Catecholase model

1. Introduction

Metalloenzymes are highly active and selective catalysts governing vital functions of living organisms. Efforts directed at understanding their mode of operation have led to development of the modeling approach, which has proved to be quite successful in tackling structural and mechanistic problems of enzyme activity. Metal complex based functional metalloenzyme models are of considerable interest both as sources of mechanistic information on enzyme reactions and as possible starting points for developing biomimetic catalysts for synthetic applications [1–7]. There has been intense activity in the study of catechol oxidase (catecholase) and dioxygenase models and their application in mild and selective bioinspired oxidations [3–11]. The corresponding enzyme reactions are involved in the metabolism of aromatic compounds, which are first converted to phenols and then to catechols. Catechol oxidases convert catechols to *o*-benzoquinones and catechol dioxygenases catalyze the oxidative cleavage of the same substrates with oxygen insertion.

Our earlier work was concerned with the biomimetic catalytic oxidation of 3,5-di-*tert*-butylcatechol (3,5-H_2dtbc), using the functional catecholase models [bis(dimethyl-glyoximato) cobalt(II)] [12–15] and [bis(dimethylglyoximato)iron(II)] [16,17] complexes (also known as cobaloxime(II) and ferroxime(II) derivatives, respectively). Kinetic investigations of these models were carried out to help elucidate the mechanism of the underlying biological catecholase reaction.

The related phenoxazinone synthase transforms aminophenols to 2-amino-3*H*-phenoxazin-3-one [9,18,19]. Cobaloxime (II) and ferroxime(II) also act as functional phenoxazinone

* Corresponding author.
E-mail address: simandi@chemres.hu (L.I. Simándi).

1381-1169/$ – see front matter © 2006 Elsevier B.V. All rights reserved.
doi:10.1016/j.molcata.2006.11.017

synthase models [18–20]. They have rigid H-bonded structures, which favor a two-step H-atom transfer mechanism exhibiting a kinetic isotope effect (KIE) [21].

A dioximatomanganese(II) dimer has recently been shown to enhance the base-catalyzed catecholase activity in MeOH via a novel type of Mn-enhanced pathway [22]. It exhibited a similar effect in the base-catalyzed phenoxazinone synthase model reaction [23].

In extension of our studies to other dioximatoiron(II) complexes, we have synthesized the new dioximatoiron(II) complexes $[Fe(Hdmed)]^+$, $[Fe(Hdmpd)]^+$ and $[Fe(H_2dmdt)]^{2+}$ and have determined their structure by X-ray scattering in methanol solution and by quantum-chemical calculations [24]. In this paper, we report the kinetics and mechanism of the catalytic oxidation of 3,5-di-*tert*-butylcatechol (H_2dtbc) by O_2, in the presence of the new complexes.

2. Experimental

The dioximato ligands $R[N{=}C(CH_3){-}C(CH_3){=}NOH]_2$, where R = $-CH_2-CH_2-$ (H_2dmed), $-CH_2-CH_2-CH_2-$ (H_2dmpd) or $-CH_2-CH_2-NH-CH_2-CH_2-$ (H_2dmdt), were prepared by condensation of diacetyl monoxime (dm) with ethylenediamine, 1,3-propylenediamine and diethylene triamine using the modified procedure of ref. [25]. The 1:1 dioximatoiron(II) complexes of these ligands, viz. $[Fe(Hdmed)](HCO_2)$, $[Fe(Hdmpd)](HCO_2)$ and $[Fe(H_2dmdt)](HCO_2)_2$ were synthesized anaerobically by the Schlenk technique as formates [24]. Good solubility in various solvents prevented crystallization, therefore, their structures were determined by X-ray scattering measurements in methanol [24]. Monocations $[Fe(Hdmed)]^+$ and $[Fe(Hdmpd)]^+$ are square-planar complexes, stabilized by strong equatorial hydrogen bonding, whereas $[Fe(H_2dmdt)]^{2+}$ is a distorted five-coordinate dication, in which H-bonding is no longer possible because of the distance between the =NOH groups (Scheme 1).

UV–vis spectra were recorded in a Hewlett-Packard 8453 diode array spectrophotometer. Mass spectra were taken in a Perkin-Elmer Sciex API 2000 instrument, using an APCI ion source, and a VG ZAB2-SEQ Tandem MS System with electron impact ionization. Electron spin resonance (ESR) spectra were recorded in a Bruker ELEXYS E500 CW EPR in methanol solution. The Mössbauer spectra of the complexes were obtained in a WISSEL type spectrometer in the transmission mode at LN temperature, using a ^{57}Co/Rh γ-source. The spectra were evaluated by the MOSSWIN program [26].

Rates of dioxygen absorption were recorded in a thermostated gas-volumetric setup (gas burette) operating at constant (atmospheric) pressure. The solid iron(II) complex was placed in a sample holder for the period of thermal equilibration under O_2 or air. The catalyst was then dropped into the solution containing the substrate. In runs with added triethylamine, it was added from a syringe through a septum simultaneously with the catalyst to avoid any oxidation during the thermostatting time. The initial rates of O_2 absorption were determined by fitting the absorption versus time (t) curves with an equation of the form $y = at/(b + t)$. The rates were then calculated from the first derivative dy/dx with excellent reproducibility.

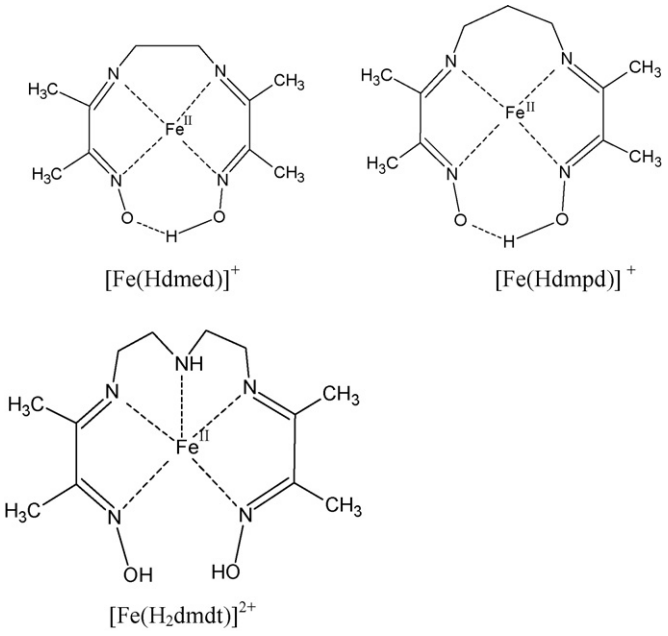

Scheme 1. Structures of catalyst complexes.

3. Results and discussion

3.1. Characterization of complexes

Additional characterization of the complexes was done by Mössbauer spectroscopy, which yielded information about the symmetry and polarity of the complexes. The isomer shift (IS) and quadrupole splitting (QS) values are shown in Table 1. The IS is indicative of the electron density at the iron nucleus, whereas QS is characteristic of the electric field inhomogeneity at the nucleus [27].

All three spectra show the presence of a predominant (>95%) component corresponding to low-spin iron(II) and a minor impurity of iron(III). The IS and QS values are nearly identical for $[Fe(Hdmed)]^+$ and $[Fe(Hdmpd)]^+$, both of which have square-planar 4N coordination spheres. The complex $[Fe(H_2dmdt)]^{2+}$ shows significantly greater IS and QS parameters, indicating that the fifth, secondary N-atom is also bonded to the central iron atom, resulting in a less symmetrical structure in line with expectations. The Mössbauer parameters are thus in agreement with the X-ray scattering and quantum-chemical results [27].

Table 1
Mössbauer parameters of the new complexes (mm s^{-1})

Complex	Isomer shift (IS)	Quadrupole splitting (QS)
$[Fe(Hdmed)]^+$	0.118	0.756
$[Fe(Hdmpd)]^+$	0.116	0.763
$[Fe(H_2dmdt)]^{2+}$	0.224	0.884

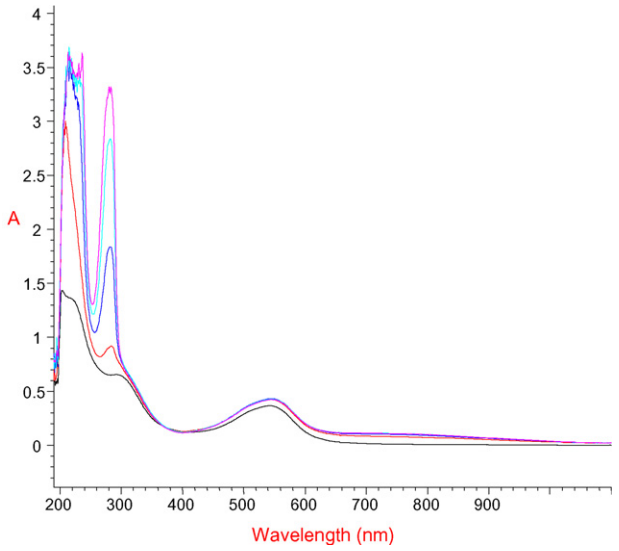

Fig. 1. Effect of increasing H_2dtbc concentration on the UV–vis spectrum of 1.06×10^{-4} M $[Fe(H_2dmdt)]^{2+}$ in N_2 atmosphere (from bottom to top $[H_2dtbc]_o = 0$, 1.06×10^{-4}, 5.30×10^{-4}, 1.06×10^{-3}, 1.59×10^{-3} M). Absorbance scale 0–3.5 AU, wavelength scale 200–900 nm.

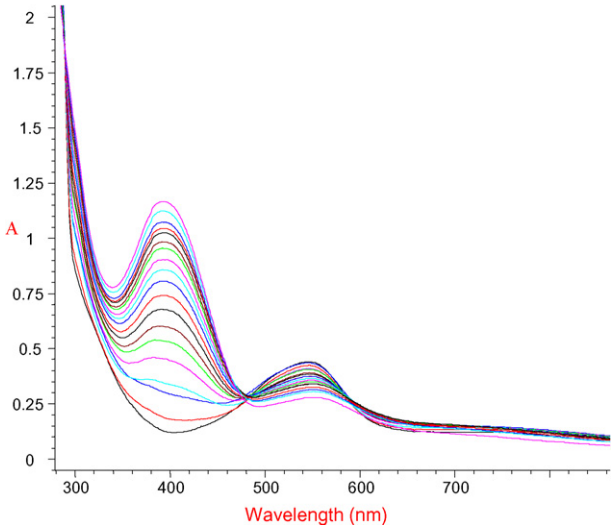

Fig. 2. Evolution of spectra upon catalytic oxidation of H_2dtbc with O_2 (air atmosphere) to the corresponding *o*-benzoquinone. Catalyst: 1.10×10^{-4} M $[Fe(H_2dmdt)]^{2+}$; $[H_2dtbc]_o = 7.90 \times 10^{-4}$ M; in MeOH, $t = 25\,^{\circ}C$, $\Delta t = 0$–150 s.

3.2. Spectroscopic monitoring of the reaction

We have found that the oxidation of 3,5-di-*tert*-butylcatechol (H_2dtbc) by O_2 is catalyzed by the dioximatoiron(II) complexes $[Fe(Hdmed)]^+$, $[Fe(Hdmpd)]^+$ and $[Fe(H_2dmdt)]^{2+}$ formed in methanol. The stoichiometry was established by monitoring the O_2 uptake by a volumetric technique [22] until absorption practically ceased. The volume of dioxygen consumed up to this point corresponded to the stoichiometric Eq. (1), i.e.

$$H_2dtbc + 0.5O_2 \rightarrow dtbq + H_2O \quad (1)$$

As the addition of H_2dtbc affects the rate of oxidation, it is important also to see its influence on the spectra under N_2 (Fig. 1). The catalytic oxidation was monitored by recording the time evolution of the UV–vis spectra. The successive spectra observed for $[Fe(H_2dmdt)]^{2+}$ as catalyst and dtbq as product are shown in Fig. 2. The appearance of isosbestic points at 480 and 590 nm indicates that a single reaction (1) involving the absorbing reactants and/or products is taking place.

The reacting solutions exhibit the ESR signal shown in Fig. 3, corresponding to the 3,5-di-*tert*-butyl-1,2-semiquinonato anion radical ($dtsq^{\bullet -}$), as supported by the simulated signal. This indicates the involvement of $dtsq^{\bullet -}$ as a reaction intermediate.

3.3. Kinetics and mechanism

3.3.1. Catalysis by iron complexes alone (without added TEA)

In order to obtain systematic kinetic information, we have selected the volumetric method, which has the advantage that the O_2 absorption rates measured by this technique are directly connected with the rate of oxidation, i.e. the formation of the dtbq product.

The initial rates of O_2 absorption (V_{in}) were measured as a function of the catalyst, substrate and dioxygen concentration.

Fig. 4 shows the initial rate (V_{in}) versus the catalyst concentration $[Fe]_o$ for $[Fe(Hdmed)]^+$, $[Fe(Hdmpd)]^+$ and $[Fe(H_2dmdt)]^{2+}$.

Fig. 5 shows the initial rate (V_{in}) as a function of the substrate concentration $[H_2dtbc]_o$ for $[Fe(Hdmed)]^+$, $[Fe(Hdmpd)]^+$ and $[Fe(H_2dmdt)]^{2+}$.

Dependence of the initial rate on the dioxygen concentration for $[Fe(Hdmed)]^+$, $[Fe(Hdmpd)]^+$ and $[Fe(H_2dmdt)]^{2+}$ is shown in Fig. 6.

According to Figs. 4–6, for all of the three catalysts, the reaction is first-order with respect to both the catalyst and dioxygen concentration, and shows saturation behavior as a function of substrate concentration. This kinetic pattern corresponds to the following empirical rate law:

$$V_k = \frac{A[Fe]_o[O_2]_o[H_2dtbc]_o}{(1 + B[H_2dtbc]_o)} \quad (2)$$

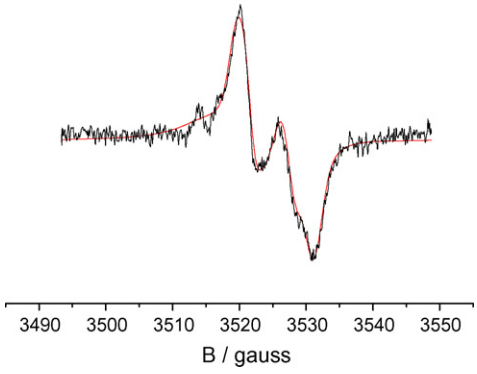

Fig. 3. Measured and simulated ESR spectra of 3,5-di-*tert*-butyl-1,2-semiquinone anion radical ($dbsq^{\bullet -}$) detected in the reacting system ($g_0 = 2.0038$, $a_H = 3.3$ G).

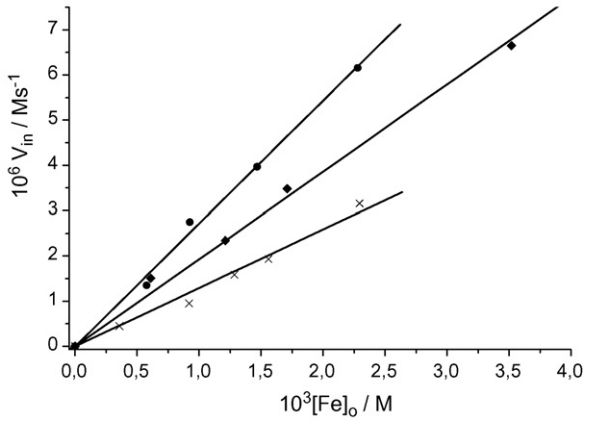

Fig. 4. Dependence of the intial rate of O_2 absorption (V_{in}) on the initial catalyst concentration $[Fe]_o$. Solvent MeOH, $T = 25\,^\circ$C. (♦) $[Fe(H_2dmdt)]^{2+}$, $[H_2dtbc]_o = 35.0$ mM; (×) $[Fe(Hdmpd)]^+$, $[H_2dtbc]_o = 23.0$ mM; (●) $[Fe(Hdmed)]^+$, $[H_2dtbc]_o = 22.9$ mM.

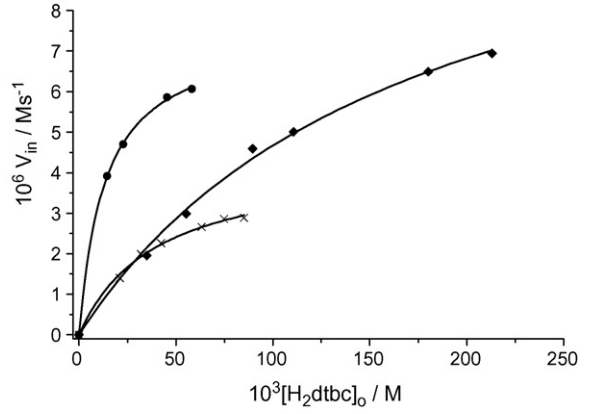

Fig. 5. Initial rate of O_2 uptake vs. initial substrate concentration. Solvent MeOH, $T = 25\,^\circ$C. (♦) $[Fe(H_2dmdt)]^{2+} = 1.21$ mM; (×) $[Fe(Hdmpd)]^+ = 1.06$ mM; (●) $[Fe(Hdmed)]^+ = 1.46$ mM.

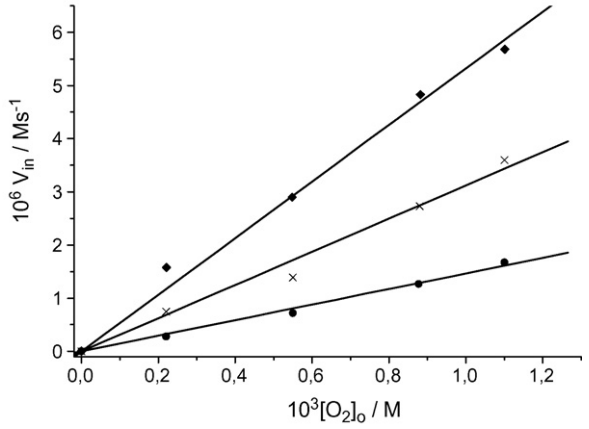

Fig. 6. Initial rate of O_2 uptake vs. equilibrium concentration of dioxygen in the solution. Solvent MeOH, $T = 25\,^\circ$C. (♦) $[Fe(H_2dmdt)]^{2+} = 1.20$ mM, $[H_2dtbc]_o = 54.9$ mM; (×) $[Fe(Hdmpd)]^+ = 1.09$ mM, $[H_2dtbc]_o = 31.5$ mM; (●) $[Fe(Hdmed)]^+ = 1.11$ mM, $[H_2dtbc]_o = 21.6$ mM.

where $[Fe]_o$ is the concentration of the iron catalyst, and A and B are constants.

The proposed reaction mechanism should be consistent with the rate law (2), taking into account the structural type of the dibasic ligand H_2L, which can be either tetradentate (H_2dmed or H_2dmpd) or pentadentate (H_2dmdt). We shall separately consider these cases below, because they imply differences due to the available coordination sites on the complexes.

In Case 1 ($H_2L = H_2$dmed or H_2dmpd), both complexes have the formula $[Fe^{II}(HL)]^+$ in solution and are four-coordinate (CN4) with square-planar geometry stabilized by hydrogen bonding between the two ends of the coordinated monoanion in the equatorial plane [24]. The axial positions are occupied by MeOH molecules (not shown).

The proposed mechanism of H_2dtbc oxidation catalyzed by these complexes consists of steps (3)–(9).

$$\underset{\text{CN4}}{[Fe^{II}(HL)]^+} + H_2\text{dtbc} \rightleftarrows \underset{\text{CN5}}{[Fe^{II}(H_2L)(\text{Hdtbc})]^+} \quad (K_1) \tag{3}$$

$$\underset{\text{CN5}}{[Fe^{II}(H_2L)(\text{Hdtbc})]^+} + O_2 \rightleftarrows \underset{\text{(X)(CN6)}}{[Fe^{III}(H_2L)(\text{Hdtbc})(O_2)]^+} \quad (K_2\} \tag{4}$$

$$X \rightarrow \underset{\text{CN5}}{[Fe^{III}(HL)(O_2H)]^+} + \text{dbsq}^{\bullet -} + H^+ \quad (\text{rds}, k_3) \tag{5}$$

$$[Fe^{III}(HL)(O_2H)]^+ \rightarrow [Fe^{II}(HL)]^+ + O_2{}^- + H^+ \quad (\text{fast}) \tag{6}$$

$$\text{dbsq}^{\bullet -} + O_2 \rightarrow \text{dtbq} + O_2{}^- \quad (\text{fast}) \tag{7}$$

$$2O_2{}^- \rightarrow O_2{}^{2-} + O_2 \quad (\text{fast}) \tag{8}$$

$$O_2{}^{2-} + H_2O \rightarrow 0.5O_2 + 2OH^- \quad (\text{fast}) \tag{9}$$

According to mechanism (3)–(9), the catecholato monoanion first binds to the four-coordinate catalyst in equilibrium (3) (cf. Fig. 1). This is accompanied with opening of the macrocycle and binding of the proton released to the oximato group. The five-coordinate intermediate binds dioxygen in the sixth position (step 4), generating the six-coordinate ternary catalyst-substrate-dioxygen intermediate X (structure in Scheme 2), which in rate-controlling step (5) eliminates $\text{dbsq}^{\bullet -}$ detected by ESR spectroscopy. The (hydrogen-peroxo)iron(III) species $[Fe^{III}(HL)(OOH)]^+$ thus formed decomposes in step (6), regenerating the starting catalyst $[Fe^{II}(HL)]^+$ and yielding $O_2{}^-$ as the first reduction product. In step (7), $\text{dbsq}^{\bullet -}$ is rapidly oxidized by O_2 to dtbq, also yielding $O_2{}^-$. Reaction (8) is the disproportionation of superoxide ion and (9) is the (catalytic) decomposition of peroxide ion regenerating some dioxygen. Reaction (8) and the repeated occurrence of (9) ensure the overall stoichiometry (1).

In Case 2 ($H_2L = H_2$dmdt), the ligand is pentadentate with 5N donor atoms. The catalyst complex is five-coordinate having the formula $[Fe^{II}(H_2\text{dmdt})]^{2+}$, i.e. the ligand remains diprotonated in the complex. The strongly distorted geometry precludes intramolecular hydrogen bonding and the formation of a macrocycle.

The proposed mechanism of H_2dtbc oxidation catalyzed by $[Fe(H_2\text{dmdt})]^{2+}$ consists of steps (10)–(13) followed by the same

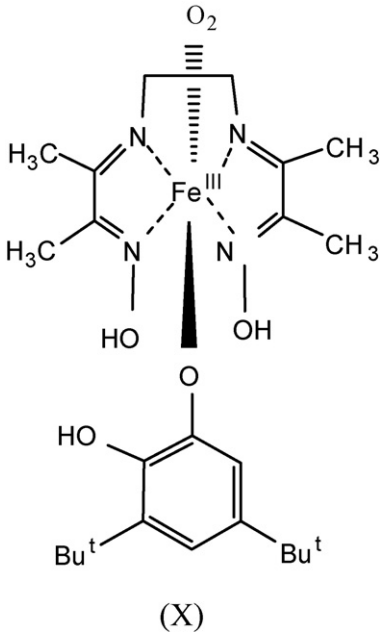

(X)

Scheme 2. Ternary intermediate X formed in reaction step (4) (Case 1).

rapid steps (7)–(9) as in Case 1. For clarity's sake, steps (10) and (11) are also illustrated by structural formulas in Scheme 3.

$$[Fe^{II}(H_2L)]^{2+} + H_2dtbc \rightleftharpoons [Fe^{II}(H_3L)(Hdtbc)]^{2+} \quad K_1 \quad (10)$$

$$[Fe^{II}(H_3L)(Hdtbc)]^{2+} + O_2 \rightleftharpoons \underset{(Y)}{[(H_3L)Fe^{III}(Hdtbc)(O_2)]^{2+}} \quad K_2 \quad (11)$$

$$Y \rightarrow [(H_2L)Fe^{III}O\text{–}OH]^{2+} + dbsq^{\bullet -} + H^+ \quad k_3 \quad \text{(slow)} \quad (12)$$

$$[(H_2L)Fe^{III}O\text{–}OH]^{2+} \rightarrow [Fe^{II}(H_2L)]^{2+} + O_2{}^- + H^+ \quad \text{(fast)} \quad (13)$$

$$dbsq^{\bullet -} + O_2 \rightarrow dtbq + O_2{}^- \quad \text{(fast)} \quad (7)$$

$$2O_2{}^- \rightarrow O_2{}^{2-} + O_2 \quad \text{(fast)} \quad (8)$$

$$O_2{}^{2-} + H_2O \rightarrow 0.5O_2 + 2OH^- \quad \text{(fast)} \quad (9)$$

As opposed to Case 1, only a single vacant coordination site is available for H_2dtbc oxidation when the five-coordinate $[Fe(H_2dmdt)]^{2+}$ is used as catalyst (Scheme 3). Nevertheless, the activity of this complex is quite similar to those of $[Fe(Hdmpd)]^+$ and $[Fe(Hdmed)]^+$, which indicates similarity of the reaction mechanisms. In view of this, we propose that the pentacoordinate $[Fe(H_2dmdt)]^{2+}$ binds H_2dtbc but, instead of ejecting a proton, binds it to the imine nitrogen. This event also generates an empty coordination site, which is capable of binding atmospheric O_2 to form the six-coordinate Fe-substrate-O_2 ternary active complex (Y). For clarity, the structural changes involved are shown in Scheme 3.

The key difference between the above mechanism and that operating in Case 1 is that here the sixth coordination site, required for O_2 binding, is vacated by proton-assisted cleavage of the Fe–NH bond. The catalyst complex is regenerated in fast step (13) together with a superoxide ion. The subsequent steps (7)–(9) are the same as in Case 1 of the four-coordinate $[Fe(Hdmed)]^+$ and $[Fe(Hdmpd)]^+$.

The rate equation for Case 1 is derived by first introducing the notations: Fe, $[(HL)Fe]^+$, the catalyst complex used: $[Fe]_o$, initial concentration of the catalyst; [Fe], free concentration of the catalyst; Fe^b, $[(H_2L)Fe(Hdtbc)]^+$, the binary (five-coordinate) mixed-ligand complex formed in equilibrium (3); Fe^t, $[(H_2L)Fe(Hdtbc)(O_2)]^+$, the active ternary (six-coordinate) intermediate formed in equilibrium (4).

Superscripts b and t refer to the binary and ternary mixed-ligand complexes.

The rate of formation of dtbq can be given by Eq. (14)

$$\frac{d[dtbq]}{dt} = V_{in} = k_3[Fe^t] \quad (14)$$

The concentration of the ternary active complex Fe^t can be expressed from prior equilibria (3) and (4) and the corresponding balance equations. The equilibrium constants K_1 and K_2 can be written approximately as Eqs. (15) and (16), because under apparent first-order conditions the substrate consumption is negligible, i.e. $[H_2dtbc] \approx [H_2dtbc]_o$. Also, owing to intense

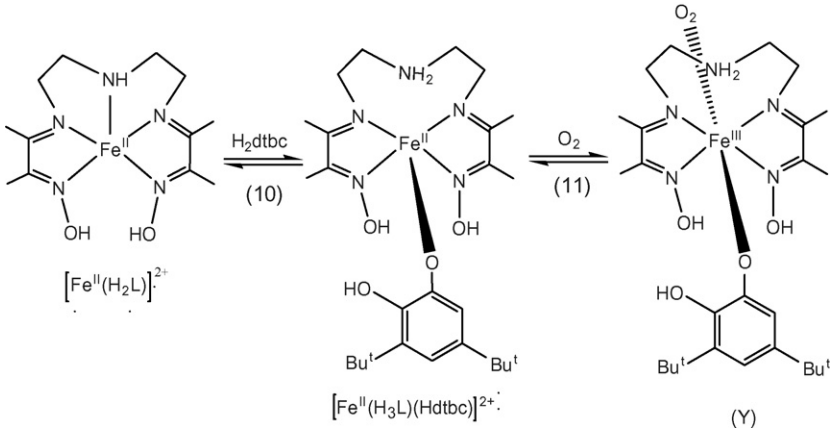

Scheme 3. Structural changes involved in the formation of active intermediate Y via steps (10) and (11).

Table 2
Kinetic parameters calculated from the substrate dependence of the rate

Catalyst complex	K_1 (M^{-1})	k_3K_2 ($M^{-1}\,s^{-1}$)	$k_3K_2K_1$ ($M^{-2}\,s^{-1}$)
$[Fe(H_2dmdt)]^{2+}$	5.86 ± 0.1	9.50 ± 0.2	55.6 ± 1.1
$[Fe(Hdmpd)]^{+}$	25.3 ± 0.5	3.70 ± 0.1	93.6 ± 1.9
$[Fe(Hdmed)]^{+}$	74.9 ± 1.5	4.67 ± 0.1	350 ± 7.0

stirring, the dioxygen concentration can be regarded as equal to the saturation value, i.e. $[O_2] \approx [O_2]_o$.

$$K_1 = \frac{[Fe^b]}{[Fe]\,[H_2dtbc]_o} \quad (15)$$

$$K_2 = \frac{[Fe^t]}{[Fe^b]\,[O_2]_o} \quad (16)$$

As a result, we obtain expression (17) for $[Fe^t]$.

$$[Fe^t] = K_2[O_2]_o[Fe^b] = K_1K_2[Fe][H_2dtbc]_o[O_2]_o \quad (17)$$

In view of the rapid decomposition of the (hydrogenperoxo)iron(III) in step (6), the approximate balance Eq. (18) is valid for the iron species involved.

$$[Fe]_o \approx [Fe] + [Fe^b] + [Fe^t] \quad (18)$$

As the concentration of the ternary complex Fe^t is negligible during the whole of the catalytic cycle, we can insert $[Fe^b]$ from Eqs. (15) into (18), which further simplifies it to Eq. (19).

$$[Fe]_o \approx [Fe] + [Fe^b] = [Fe](1 + K_1[H_2dtbc]_o) \quad (19)$$

Upon insertion of $[Fe^t]$ from (17) into Eq. (14), we obtain the final rate Eq. (20) for Case 1.

$$V_{in} = \frac{k_3K_1K_2[Fe]_o[O_2]_o[H_2dtbc]_o}{1 + K_1[H_2dtbc]_o} \quad (20)$$

As the structure of Eq. (20) is identical with that of Eq. (2), the observed kinetic behavior is consistent with the proposed mechanism (3)–(9) (Case 1).

The rate of oxidation in Case 2 can be written in a way identical to that applied in Case 1, i.e. as the rate of decomposition of the ternary complex Fe^t given by Eq. (14). Upon further rearrangements, (14) takes the form of Eq. (20).

The kinetic parameters of the reactions can be determined by fitting Eq. (20) to the dependences of the initial rate V_{in} on the catalyst, dioxygen and substrate concentration curves shown in Figs. 4–6, respectively.

It is convenient first to evaluate the substrate dependence (Fig. 5), which can be written as a function of two parameters, P_1 and P_2. From P_1, we can obtain k_3K_2, and P_2 is identical with K_1, i.e. both independent parameters are available from the substrate dependence of the initial rate.

These results are listed in Table 2. The dependences on the catalyst and dioxygen concentration are shown in Figs. 4 and 6 for the three catalysts. These results are also consistent with the proposed mechanism: the slopes of the linear plots calculated from the parameters obtained from Fig. 5 are in good agreement with the experimental results (Tables 2 and 3).

Table 3
Comparison of the measured and calculated slopes (s^{-1}) of the dependence of rate on catalyst and dioxygen concentration for the three complexes studied

	10^3 slope	
	(V_{in} vs. $[Fe]_o$)	(V_{in} vs. $[O_2]_o$)
$[Fe(H_2dmdt)]^{2+}$		
Calculated	1.78	4.78
Measured	1.86	5.05
$[Fe(Hdmpd)]^{+}$		
Calculated	1.50	1.79
Measured	1.36	1.52
$[Fe(Hdmed)]^{+}$		
Calculated	3.04	3.20
Measured	2.72	3.20

The reactivity trends in the absence of TEA, reflected by Table 2 deserve attention. There is a parallel correlation between the stability constant of the catalyst-substrate complex (K_1) and the overall catalytic activity defined by the product $k_3K_2K_1$. This trend seems to follow the increase in the rigidity of the catalyst complex in the series $[Fe(H_2dmdt)]^{2+} < [Fe(Hdmpd)]^{+} < [Fe(Hdmed)]^{+}$. The pentacoordinate ferroxime(II), $[Fe(Hdmg)_2MeIm]$, studied earlier [16], is more reactive than any of the catalysts used in this work, in accordance with the rigidity (hardness) pattern.

3.3.2. Catalysis by iron complexes with added TEA

We have observed that the addition of TEA to methanol solutions of $[Fe(H_2dmdt)]^{2+}$, $[Fe(Hdmpd)]^{+}$ and $[Fe(Hdmed)]^{+}$ considerably accelerates the catalytic oxidation of H_2dtbc to the corresponding 1,2-benzoquinone (dtbq). When TEA is added to a solution in which the Fe-catalyzed catecholase reaction is in progress, a strong acceleration of dtbq formation is observed (Fig. 7).

In the detailed study of this effect, TEA has remained the base of choice because of its strength ($pK_a = 9.73$ [28]). Strong inorganic bases (NaOH, KOH) were avoided to prevent decomposition of the complexes, whereas weaker organic bases like

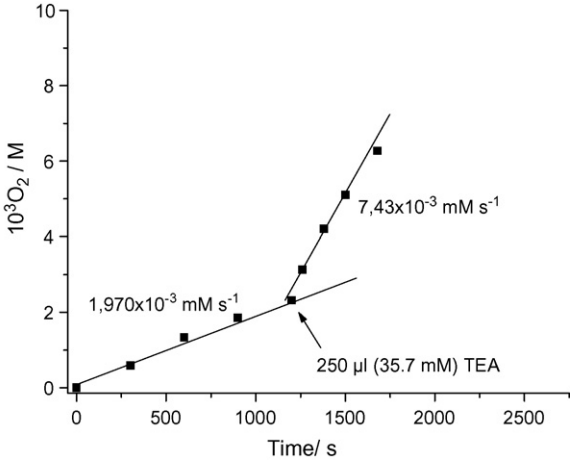

Fig. 7. Acceleration of O_2 uptake upon addition of TEA to the reacting solution.

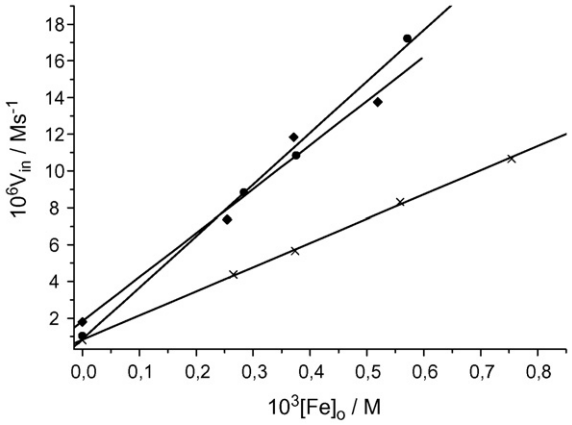

Fig. 8. Initial rate of O_2 uptake vs. initial catalyst concentration in the presence of 7.17 mM TEA. Solvent MeOH, $T = 25\,^{\circ}C$. (♦) $[Fe(H_2dmdt)]^{2+} = 1.20$ mM, $[H_2dtbc]_o = 25.3$ mM; (×) $[Fe(Hdmpd)]^{+} = 1.09$ mM, $[H_2dtbc]_o = 26.3$ mM; (●) $[Fe(Hdmed)]^{+} = 1.11$ mM, $[H_2dtbc]_o = 28.6$ mM.

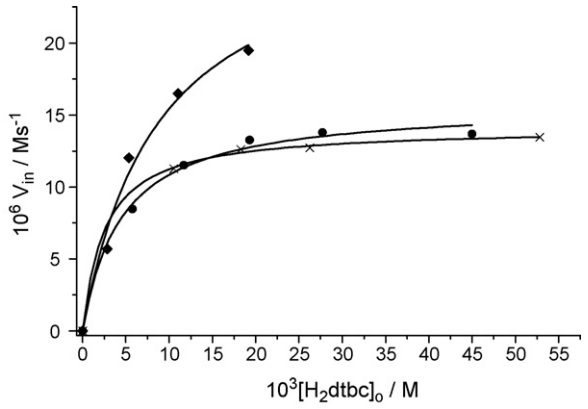

Fig. 10. Initial rate of O_2 uptake vs. initial substrate concentration in the presence of 7.17 mM TEA. Solvent MeOH, $T = 25\,^{\circ}C$. (♦) $[Fe(H_2dmdt)]^{2+} = 0.546$ mM; (×) $[Fe(Hdmpd)]^{+} = 0.534$ mM; (●) $[Fe(Hdmed)]^{+} = 0.564$ mM.

pyridine or 1-methylimidazol produced only insignificant acceleration.

The base-catalyzed autoxidation of substituted phenols and diphenols (e.g. 3,5-di-*tert*-butylcatechol) to the corresponding *o*-benzoquinone derivative is a well known reaction [4], requiring a correction when the oxidation is followed in the presence of both a catalyst and a base. The initial rates of O_2 uptake measured in the presence of TEA exhibited a behavior similar to those runs recorded without TEA, but the rates measured were greater by about an order of magnitude. First-order dependences were observed on the initial catalyst and dioxygen concentration (Figs. 8 and 9), whereas saturation curves were obtained as a function of both initial substrate and TEA concentration (Figs. 10 and 11, respectively).

The kinetic behavior of H_2dtbc oxidation in the presence of TEA differs from the TEA-free system in the following features. (a) The TEA (base)-catalyzed oxidation of H_2dtbc takes place via deprotonation and oxygenation to the hydroperoxo species $HdtbcO_2^-$ [22,23], followed by elimination of $dtsq^{-\bullet}$. (b) The major (fastest) oxidation path is the Fe-assisted route, in which $HdtbcO_2^-$ is coordinated to the Fe^{II} species, yielding the hydroperoxo intermediates $[Fe^{II}(Hdmed)(HdtbcO_2^-)]$, $[Fe^{II}(Hdmpd)(HdtbcO_2^-)]$ and $[Fe^{II}(H_2dmdt)(HdtbcO_2^-)]^+$. Each of these species can eliminate $dtsq^{\bullet-}$, leading to substrate oxidation to dtbq. (c) In principle, the oxidation of H_2dtbc catalyzed by the Fe^{II} complexes without participation of TEA may still occur although to a negligible extent only.

The overall initial rate of catechol oxidation (V_{in}) can thus be expressed as the sum of three terms, viz.

$$V_{in} = \underset{(a)}{V_{TEA}} + \underset{(b)}{V_{Fe\text{-}TEA}} + \underset{(c)}{V_{Fe}} \quad (21)$$

The relative importance of contributing paths has been investigated by comparing the rates observed (V_{in}) under three sets of conditions (Table 4).

Considering the data in Table 4, path c can safely be neglected in the presence of added TEA, therefore, the overall rate is the sum of contributions by the TEA-catalyzed (V_{TEA}) and Fe-

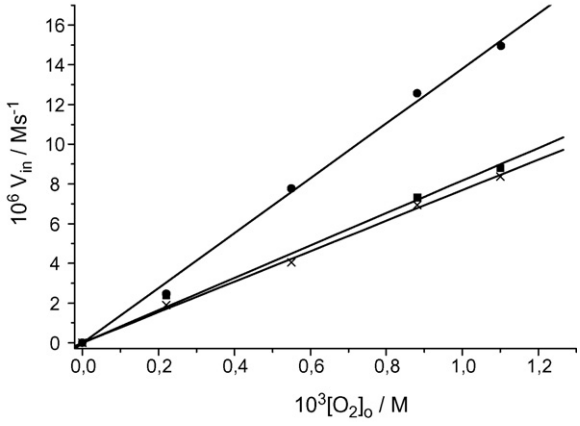

Fig. 9. Initial rate of O_2 uptake vs. equilibrium concentration of dioxygen in the solution, In the presence of 7.17 mM TEA. Solvent MeOH, $T = 25\,^{\circ}C$. (♦) $[Fe(H_2dmdt)]^{2+} = 0.494$ mM, $[H_2dtbc]_o = 10.2$ mM; (×) $[Fe(Hdmpd)]^{+} = 0.532$ mM, $[H_2dtbc]_o = 10.4$ mM; (●) $[Fe(Hdmed)]^{+} = 0.548$ mM, $[H_2dtbc]_o = 10.8$ mM.

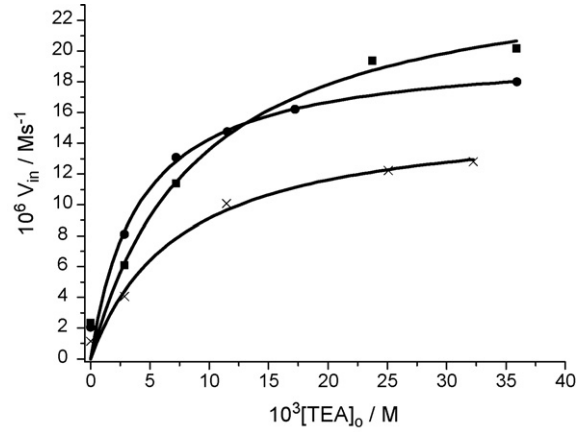

Fig. 11. Initial rate of O_2 uptake vs. initial TEA concentration. Solvent MeOH, $T = 25\,^{\circ}C$. (♦) $[Fe(H_2dmdt)]^{2+} = 0.986$ mM, $[H_2dtbc]_o = 11.5$ mM; (×) $[Fe(Hdmpd)]^{+} = 1.15$ mM, $[H_2dtbc]_o = 11.4$ mM; (●) $[Fe(Hdmed)]^{+} = 1.14$ mM, $[H_2dtbc]_o = 11.3$ mM.

Table 4
Contribution of the three possible reaction paths to the overall rate of H_2dtbc oxidation in the presence of TEA

Path	Conc. of $[Fe(dmed)]^+$ (mM)	$[TEA]_o$ (mM)	$[H_2dtbc]$ (mM)	Initial rate (V_{in}) (mM s^{-1})	Fig. no.
(a) TEA catalyzed	0.0	7.17	23.0	1.25	Calcd. (TEA only)
(b) Fe-enhanced	0.5	7.17	28.64	14.2	Fig. 8 (●) (major route)
(c) Fe only	0.5	0.0	22.86	1.2	Fig. 4 (●) (negligible)

enhanced ($V_{Fe\text{-}TEA}$) rates.

$$V_{in} \approx V_{TEA} + V_{Fe\text{-}TEA} \quad (22)$$

The reaction mechanism in the presence of TEA can be written as Eqs. (23)–(34) (superscript and subscript T refer to TEA), depending on the ligand structure. In Case 1 ($H_2L = H_2$dmed or H_2dmpd), both ligands are tetradentate.

$$H_2dtbc + TEA \rightleftarrows Hdtbc^- + HTEA^+ \quad K = K_C/K_T \quad (23)$$

$$Hdtbc^- + O_2 \rightleftarrows HdtbcO_2^- \quad K_B \quad (24)$$

$$HdtbcO_2^- \rightarrow dbsq^{\bullet -} + HO_2 \quad k_B \quad (25)$$

$$HO_2 + TEA \rightleftarrows O_2^- + HTEA^+ \quad (fast) \quad (26)$$

$$dbsq^{\bullet -} + O_2 \rightarrow dtbq + O_2^- \quad (fast) \quad (27)$$

$$[(HL)Fe^{II}]^+ + HdtbcO_2^- \rightleftarrows [(HL)Fe^{III}(O_2dtbcH)] \quad K_1^T \quad (28)$$

$$[(HL)Fe^{III}(O_2dtbcH)] \rightarrow [(HL)Fe^{III}(O_2H)]^+ + dbsq^{\bullet -} \quad k_{Fe} \quad (29)$$

$$[(HL)Fe^{III}(O_2H)]^+ \rightarrow [(HL)Fe^{II}]^+ + O_2^- + H^+ \quad (fast) \quad (30)$$

$$[(HL)Fe^{II}]^+ + Hdtbc^- \rightleftarrows [(HL)Fe^{II}(Hdtbc)] \quad K_{bin} \quad (31)$$

$$[(HL)Fe^{II}(Hdtbc)] + O_2 \rightleftarrows [(HL)Fe^{III}(Hdtbc)(O_2)] \quad K_{ter} \quad (32)$$

$$2O_2^- \rightarrow O_2^{2-} + O_2 \quad (fast) \quad (33)$$

$$O_2^{2-} + H_2O \rightarrow 0.5O_2 + 2OH^- \quad (fast) \quad (34)$$

In the above mechanism, (23)–(27) represent the base-catalyzed path, specifically (23) is a proton exchange equilibrium. Step (24) is O_2 binding to the catecholate(1-), affording a hydroperoxide ion, which eliminates $dbsq^{\bullet -}$ in (25). Alternatively, $HdtbcO_2^-$ binds to $[Fe^{II}(HL)]^+$ in (28). The ternary reactive intermediate thus formed loses $dbsq^{\bullet -}$ faster in rate-controlling step (29) than does $HdtbcO_2^-$ in (25). This is the source of the Fe-enhanced catecholase reaction. The structural changes are shown in Scheme 4. The product dtbq is formed in the known rapid oxidation of $dbsq^{\bullet -}$ (27). The primary reduction product O_2^- is ultimately reduced to OH^- via (33) and (34). Equilibria (31) and (32) are non-productive equilibria with low conversion and excessive steric hindrance against product formation.

A slightly modified version of the above mechanism is valid in Case 2, when $H_2L = H_2$dmdt (pentadentate). It can be obtained by replacing $[Fe^{II}(HL)]^+$ with $[Fe^{II}(H_2L)]^{2+}$ and adjusting the differences in charges. Also, equilibrium (32) should be omitted, as it would lead to a seven-coordinate complex as product.

3.3.3. Derivation of the kinetic equation

The kinetic equation for both Cases 1 and 2 of mechanism (23)–(34) can be obtained by inserting the rate terms $V_{TEA} + V_{Fe\text{-}TEA}$ into Eq. (22).

$$V_{in} = V_{TEA} + V_{Fe\text{-}TEA} = (k_B + k_{Fe}^T K_1^T [Fe]_o)\, K_B [Hdtbc^-][O_2]_o \quad (35)$$

Here, $[Fe]_o$ is the overall concentration of either $[Fe^{II}(HL)]^+$ or $[Fe^{II}(H_2L)]^{2+}$.

We need an expression for $[Hdtbc^-]$ in the reacting solution, which can be derived as follows.

The equilibrium constant for reaction (23), in combination with the balance equations for H_2dtbc and TEA yields Eqs. (36) and (37). Upon insertion of these expressions into charge balance (38), we obtain the implicit expression (39) for $[H^+]$, which can be used to obtain Eq. (40) for $[Hdtbc^-]$.

$$[Hdtbc^-] = \frac{[H_2dtbc]_o}{(1 + K_c[H^+])} \quad (36)$$

$$[HTEA^+] = \frac{[TEA]_o K_T [H^+]}{(1 + K_T[H^+])} \quad (37)$$

$$[Hdtbc^-] = [HTEA^+] \quad (38)$$

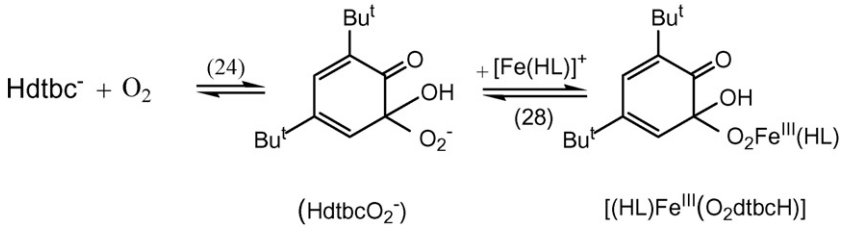

Scheme 4. Structural changes in the Fe-enhanced, base-catalyzed oxidation of H_2dtbc via steps (24) and (28).

Table 5
Cumulative rate constants $k_{Fe}^{T}K_1^{T}K_B$ ($M^{-2}\,s^{-1}$) for the complexes in the presence of TEA, calculated from the substrate dependence of the initial rate

Complex	$10^{-3}k_{Fe}K_1^{T}K_B$ ($M^{-2}s^{-1}$)
$[Fe(H_2dmdt)]^{2+}$	3.79 ± 0.08
$[Fe(Hdmpd)]^{+}$	3.29 ± 0.08
$[Fe(Hdmed)]^{+}$	6.75 ± 0.15

$$[H^+] = \frac{[H_2dtbc]_o}{K_T[TEA]_o}\,\frac{1+K_T[H^+]}{1+K_C[H^+]} \tag{39}$$

$$[Hdtbc^-] = \frac{[H_2dtbc]_o}{1+(K_C[H_2dtbc]_o/K_T[TEA]_o)((1+K_C[H^+])/(1+K_T[H^+]))} \tag{40}$$

Assuming that $K_T[H^+] \ll 1$ and $K_C[H^+] \ll 1$, Eq. (40) simplifies to (41).

$$[Hdtbc^-] = \frac{[H_2dtbc]_o}{1+(K_C[H_2dtbc]_o/K_T[TEA]_o)} \tag{41}$$

Upon substitution of $[Hdtbc^-]$ from Eq. (41) into (35), the rate equation rearranges to (42).

$$V_{in} = \frac{(k_B + k_{Fe}K_1^{T}[Fe]_o)K_B[Hdtbc^-]_o[O_2]_o}{1+(K_C[H_2dtbc]_o/K_T[TEA]_o)} \tag{42}$$

The kinetic parameter to be determined is $k_{Fe}K_BK_1^{T}$, which is characteristic of the catalytic oxidation in the presence of a given iron(II) complex. From our previous study, the rate constant for the base-catalyzed oxidation $k_B = 0.84\,M^{-1}\,s^{-1}$ and $K_C/K_T = 1.73$ [22].

The cumulative rate constants $k_{Fe}^{T}K_BK_1^{T}$ for the iron(II) complexes studied are listed in Table 5.

The results presented show that the proposed mechanisms are consistent with the observed kinetic behavior both in the absence and presence of added TEA.

The cumulative rate constants in Table 5 are within a factor of about 2, with $[Fe(Hdmed)]^+$ being favored over the other two complexes. This narrow range of reactivities is in line with the close similarity of mechanism, involving iron-enhanced base catalysis with hydroperoxide formation from $Hdtbc^-$ and O_2. This oxidation path is favored over the one occurring without base: the reactivity ratios in favor of the iron-enhanced, base-catalyzed route are 68, 35 and 19 for $[Fe(H_2dmdt)]^{2+}$, $[Fe(Hdmpd)]^+$ and $Fe(Hdmed)]^+$, respectively.

The base-catalyzed oxidation of catechols in protic solvents has been known to show features different from those of its metal complex catalyzed analogs in non-protic solvents. Studies of the latter systems have usually been undertaken to avoid undesired base-catalyzed side reactions encountered in the presence of base, specifically hydroxide ions.

In this work, we have carried out detailed kinetic studies of functional catecholase models consisting of dioximatoiron(II) complexes, using H_2dtbc as model substrate. The kinetics were followed in methanol in the presence and absence of TEA.

The results of this effort generated a novel interpretation of the catecholase reaction in methanol, in terms of a mechanism that might best be termed 'metal complex enhanced' base catalysis' of oxidation. We have first demonstrated this pathway for the TEA-catalyzed, Mn-enhanced catecholase reaction using the dioximatomanganese (II) dimer $[Mn_2(Hdmdt)_2]^{2+}$ [22]. Subsequently, the phenoxazinone synthase model reaction promoted by the same Mn-dimer was shown to follow a similar route [23].

The present dioximatoiron(II) complexes combined with TEA in MeOH offer a slightly different, but basically similar system. Whereas $[Mn_2(Hdmdt)_2]^{2+}$ alone was catalytically inactive, the dioximatoiron(II) complexes exhibited a definite catecholase activity without added TEA. This remarkable reaction was much slower though, but undoubtedly took place in the absence of TEA. The interpretation of the underlying mechanisms was straightforward for the four-coordinate $[Fe(Hdmed)]^+$ and $[Fe(Hdmpd)]^+$ complexes, where two vacant coordination sites were available for the incoming catecholato and dioxygen ligands. The lack of a vacant position in the five-coordinate $[Fe(H_2dmdt)]^{2+}$, however, imposed an obstacle for the incoming O_2 ligand, entering after $Hdtbc^-$. The only conceivable way to overcome this problem is to assume that the central NH group of the ligand temporarily vacates its site for the incoming superoxo ligand.

The same systems in the presence of TEA were accelerated by more than an order of magnitude (Table 5) relative to the TEA-free systems. Remarkably, the three complexes reacted at almost the same rates (within a factor of about 2), indicating the similarity of mechanisms. The proposed mechanism of Fe-enhanced, base-catalyzed oxidation is essentially identical for all of the three catalysts, which is in line with the observed kinetic behavior. The sole involvement of a single free coordination position on the Fe complex in the oxidation implies closely similar reactivities, which is indeed the case.

Work is in progress to further explore the scope of metal ion-enhanced base-catalyzed catechol oxidation.

Acknowledgements

This work was supported by the Hungarian Science Fund (Grants OTKA 60241 and 34282) and COST D21 Action, Metalloenzymes and model compounds.

References

[1] J. Reedijk, E. Bouwman (Eds.), Bioinorganic Catalysis, second ed., Marcel Dekker, New York, 1999.
[2] E.I. Solomon, U.M. Sundaram, T.E. Machonkin, Chem. Rev. 96 (1996) 2563.
[3] L. Que Jr., J. in, E. Reedijk, Bouwman (Eds.), Bioinorganic Catalysis, second ed., Marcel Dekker, New York, 1999, pp. 269–321 (Ref. 1).
[4] L.I. Simándi, Catalytic Activation of Dioxygen by Metal Complexes, Kluwer Academic Publishers, Dordrecht, Boston, London, 1992, p. 400.
[5] L.I. Simándi (Ed.), Advances in Catalytic Activation of Dioxygen by Metal Complexes, Kluwer Academic Publishers, Dordrecht, Boston, London, 2003, p. 336.
[6] T. Funabiki, L.I. in, Simándi (Eds.), Advances in Catalytic Activation of Dioxygen by Metal Complexes, Kluwer Academic Publishers, Dordrecht, Boston, London, 2003, pp. 158–226.

[7] O. Gentschev, N. Moller, B. Krebs, Inorg. Chim. Acta 300 (2000) 442.
[8] M. Merkel, F.K. Muller, B. Krebs, Inorg. Chim. Acta 337 (2002) 308.
[9] L.I. Simándi, T.M. Simándi, Z. May, G. Besenyei, Coord. Chem. Rev. 245 (2003) 87.
[10] R. Than, A.A. Feldmann, B. Krebs, Coord. Chem. Rev. 182 (1999) 211.
[11] C. Gerdemann, C. Eicken, B. Krebs, Acc. Chem. Res. 35 (2002) 183.
[12] L.I. Simándi, T.M. Barna, Gy. Argay, T.M. Simándi, Inorg. Chem. 34 (1995) 6337.
[13] L.I. Simándi, T.L. Simándi, J. Mol. Catal. A: Chem. 117 (1997) 299.
[14] L.I. Simándi, T.M. Simándi, J. Chem. Soc. Dalton Trans. (1998) 3275.
[15] T.L. Simándi, L.I. Simándi, React. Kinet. Catal. Lett. 65 (1998) 301.
[16] T.L. Simándi, L.I. Simándi, J. Chem. Soc., Dalton Trans. (1999) 4529.
[17] L.I. Simándi, T.L. Simándi, J. Inorg. Biochem. 86 (2001) 432.
[18] L.I. Simándi, T.M. Barna, L. Korecz, A. Rockenbauer, Tetrahedron Lett. 34 (1993) 717.
[19] L.I. Simándi, T.M. Barna, S. Németh, J. Chem. Soc. Dalton Trans. (1996) 473.
[20] T.M. Simándi, L.I. Simándi, M. Győr, A. Rockenbauer, Á. Gömöry, Dalton Trans. (2004) 1056.
[21] T.M. Simándi, L.I. Simándi, Z. May, I.Cs. Szigyártó, Dalton Trans. (2005) 365.
[22] I.Cs. Szigyártó, L.I. Simándi, L. Párkányi, L. Korecz, G. Schlosser, Inorg. Chem. 45 (2006) 7480.
[23] I.Cs. Szigyártó, T.M. Simándi, L.I. Simándi, L. Korecz, N. Nagy, J. Mol. Catal. A: Chem. 251 (2006) 270.
[24] T. Megyes, Z. May, G. Schubert, T. Grósz, L.I. Simándi, T. Radnai, Inorg. Chim. Acta 359 (2006) 2329.
[25] S. Singh, V. Chakkravorty, K.C. Dash, Indian J. Chem. Soc. Sect. A 28 (1998) 255.
[26] Z. Klencsár, E. Kuzmann, Z. Németh, J. Radioanal. Nucl. Chem. 210 (1996) 105.
[27] A. Vértes, L. Korecz, K. Burger, Mössbauer Spectroscopy Akadémiai Kiadó, Budapest and Elsevier, Lausanne, 1979.
[28] A.E. Martell, Stability Constants of Metal-Ion Complexes, Section II, Organic Ligands, Chemical Society Special Publication No. 17, The Chemical Society, London, 1964.